JOURNAL OF VIROLOGY, Aug. 2008, p. 8149–8160 Vol. 82, No. 16
0022-538X/08/$08.00+0 doi:10.1128/JVI.00047-08


# Effective Chemokine Secretion by Dendritic Cells and Expansion of Cross-Presenting CD4$^-$/CD8$^+$ Dendritic Cells Define a Protective Phenotype in the Mouse Model of Coxsackievirus Myocarditis$^\nabla$

Andreas Oliver Weinzierl,[1,2] Gudrun Szalay,[1] Hartwig Wolburg,[1] Martina Sauter,[1] Hans-Georg Rammensee,[2] Reinhard Kandolf,[1] Stefan Stevanović,[2] and Karin Klingel[1]*

*Department of Molecular Pathology, University of Tübingen, Liebermeisterstrasse 8, 72076 Tübingen, Germany,[1] and Department of Immunology, Institute for Cell Biology, University of Tübingen, Auf der Morgenstelle 15, 72076 Tübingen, Germany[2]*

Received 8 January 2008/Accepted 29 May 2008

**Enteroviruses such as coxsackievirus B3 (CVB3) are able to induce lethal acute and chronic myocarditis. In resistant C57BL/6 mice, CVB3 myocarditis is abrogated by T-cell-dependent mechanisms, whereas major histocompatibility complex (MHC)-matched permissive A.BY/SnJ mice develop chronic myocarditis based on virus persistence. To define the role of T-cell-priming dendritic cells (DCs) in the outcome of CVB3 myocarditis, DCs were analyzed in this animal model in the course of CVB3 infection. In both mouse strains, DCs were found to be infectible with CVB3; however, formation of infectious virions was impaired. In DCs derived from C57BL/6 mice, significantly higher quantities of interleukin-10 (IL-10) and the proinflammatory cytokines IL-6 and tumor necrosis factor alpha were measured compared to those from A.BY/SnJ mice. Additionally, the chemokines interferon-inducible protein 10 (IP-10) and RANTES were secreted by DCs from resistant C57BL/6 mice earlier in infection and at significantly higher levels. The protective role of IP-10 in CVB3 myocarditis was confirmed in IP-10$^{-/-}$ mice, which had increased myocardial injury compared to the immunocompetent control animals. Also, major differences in resistant and permissive mice were found in DC subsets, with C57BL/6 mice harboring more cross-priming CD4$^-$ CD8$^+$ DCs. As CD4$^-$ CD8$^+$ DCs are known to express 10 times more Toll-like receptor 3 (TLR3) than other DC subsets, we followed the course of CVB3 infection in TLR3$^{-/-}$ mice. These mice developed a fulminant acute myocarditis and secreted sustained low amounts of type I interferons; secretion of IP-10 and RANTES was nearly abrogated in DCs. We conclude that MHC-independent genetic factors involving DC-related IP-10 secretion and TLR3 expression are beneficial in the prevention of chronic coxsackievirus myocarditis.**

*Coxsackievirus* B3 (CVB3) is a positive, single-strand RNA virus of the *Picornaviridae* family. As with other enteroviruses, it can induce a wide variety of acute and chronic forms of diseases ranging from meningitis and pancreatitis to myocarditis (33). Although enteroviral infections are common and normally well-controlled by the immune system of the host, severe acute infections can lead to sudden cardiac death (3). Moreover, chronic myocarditis and also dilated cardiomyopathy may develop which can, in its end stage, only be treated by heart transplantation (22). Chronic forms of myocarditis, which are triggered by virus persistence, indicate that the cytolytic CVB3 can evade host immune surveillance. Several immunocompetent mouse strains (e.g., A.BY/SnJ, A/J, and SWR/J) develop a chronic form of myocarditis upon CVB3 infection, whereas other strains (129SvJ and C57BL/6) overcome CVB3 infection during the acute phase (25). It has been shown that type I interferon signaling (46) as well as effectual triggering of a potent CD8$^+$ T-cell response (26) are crucial for efficient CVB3 elimination. As the outcome of a CVB3 myocarditis is independent of the major histocompatibility complex (MHC) type and therefore not solely dependent to the ability of recognizing distinct CVB3 T-cell epitopes, an adequate efficiency of T-cell priming might be important for the resolution of this disease.

The cells most potent in antigen presentation, and thus also in T-cell priming, are dendritic cells (DCs) (5), which can be further subdivided into three main populations in the mouse (CD4$^+$ CD8$^-$, CD4$^-$ CD8$^+$, and CD4$^-$ CD8$^-$) (41). Myeloid CD4$^+$ CD8$^-$ DCs are effective in CD4$^+$ T-cell activation (37) and cytokine production (38), whereas CD4$^-$ CD8$^+$ DCs are most competent in cross-presentation to CD8$^+$ T cells and their activation (11, 40). Furthermore, plasmacytoid DCs (pDCs), which only assume a typical DC morphology and function after activation (35), represent the major type I interferon-producing cells in response to viral stimulation (2, 34). All DCs express a wide variety of toll-like receptors (14) that recognize various forms of viral RNA (1, 12, 32, 45). Apart from T-cell priming, DCs are also major sources of proinflammatory and antiviral cytokines and chemokines (42) and thus can direct T-helper cells ($T_h$) toward a $T_h1$ or $T_h2$ response. Based on comparisons of the interactions of different RNA viruses with DCs, rather divergent observations have been made in the past few years. Dengue virus can infect DCs and induce DC maturation, as well as the secretion of alpha interferon (IFN-α) and tumor necrosis factor alpha (TNF-α) (18). Also, severe acute respiratory syndrome (SARS) coronavirus was found to infect DCs, but the formation of infectious particles was blocked and type I interferons were secreted in only low

* Corresponding author. Mailing address: Department of Molecular Pathology, University of Tübingen, Liebermeisterstrasse 8, 72076 Tübingen, Germany. Phone: 49 7071 29 84925. Fax: 49 7071 29 5334. E-mail: karin.klingel@med.uni-tuebingen.de.

$^\nabla$ Published ahead of print on 11 June 2008.

amounts (28). In contrast, Ebola, Marburg, and Lassa viruses were shown to replicate unopposed in DCs, but no DC maturation or interferon secretion was measured (4, 7).

Based on the exceptional functions of DCs in T-cell priming and immune surveillance, we hypothesized that DCs might play a major role in eliciting a potent anti-CVB3 response, thus preventing a persistent type of infection. Hence, we compared the phenotype and functionality of DCs in permissive A.BY/SnJ mice and resistant C57BL/6 mice with regards to their influence on the course of CVB3 infection.

## MATERIALS AND METHODS

**Mice.** A.BY/SnJ (A.BY-H2$^{b}$ H2-T18$^{f}$/SnJ), IP-10$^{-/-}$ (B6.129S4-Cxcl10$^{tm1Adl}$/J), and TLR3$^{-/-}$ (B6; 129S1-Tlr3$^{tm1Flv}$/J) mice were originally purchased from Jackson Laboratories (Bar Harbor, ME). Breeding colonies of these animals were maintained at the Department of Immunology, University of Tübingen, in a specific-pathogen-free animal facility. C57BL/6 (C57BL/6NCrl *H-2*$^{b}$) mice were purchased from Charles River (Sulzfeld, Germany). Mice were used for experiments at the age of 4 to 5 weeks; all organs were removed aseptically and partially fixed in 4% buffered paraformaldehyde or frozen in liquid nitrogen until use. In general, analyses were performed individually for every animal of an experimental group. All experiments were performed according to the German animal protection law.

**Virus and immunization protocol.** Transfection-derived CVB3 (Nancy strain) (21) was prepared and purified as described previously (25). Mice were infected by intraperitoneal injection of 200 μl phosphate-buffered saline (PBS) containing $1 \times 10^5$ PFU of purified CVB3. For antigen preparation, heat inactivation of CVB3 was performed at 60°C for 15 min.

**Cell preparation from spleens.** Spleens were removed aseptically, cut into pieces, digested with 400 U collagenase D (Sigma-Aldrich, Seelze, Germany) for 30 min at 37°C, and pressed through a 40-μm cell strainer (BD Biosciences, Heidelberg, Germany) to produce single-cell suspensions. Erythrocytes were lysed using ACK lysing buffer (Lonza, Verviers, Belgium). After washing with PBS, cells were counted and resuspended in PBS supplemented with 2 mM EDTA and 0.5% bovine serum albumin. DCs were isolated using CD11c microbeads (Miltenyi Biotech, Bergisch Gladbach, Germany); pDCs were isolated with anti-mPDCA microbeads (Miltenyi Biotech, Bergisch Gladbach, Germany) as described by the manufacturer. In order to increase purity of DC isolates, positive magnetic-activated cell sorter selection was performed twice. Viability and purity of the isolated cells was assessed by fluorescence-activated cell sorter (FACS) analysis. The viability of pDCs and DCs was above 75%, and CD11c$^{+}$ cells were of >95% purity. pDCs revealed more than 60% purity; mPDCA-negative splenocytes were used as controls in pDC experiments.

**FACS analysis and sorting.** Splenocytes or purified DCs were surface stained for 20 min at 4°C with combinations of fluorescence-conjugated monoclonal antibodies: anti-CD11c–fluorescein isothiocyanate (FITC), anti-CD4–phycoerythrin (PE), anti-CD11b–PE, anti-CD14–PE, anti-CD80–PE, anti-CD86–PE, anti-H2-A–PE, anti-B220–PE, anti-CD8–allophycocyanin (APC), anti-CD11b–APC, anti-Dx5–PE, and F4/80-APC (BD Biosciences, Heidelberg, Germany) or with anti-mPDCA–APC (Miltenyi Biotech, Bergisch Gladbach, Germany). Appropriate isotype controls were used for all antibodies. After washing three times, cells were resuspended in FACS buffer (PBS, 2% bovine serum albumin, 2 mM EDTA) and analyzed on a four-color FACSCalibur apparatus (BD Biosciences, Heidelberg, Germany). Dead cells were excluded from the analysis by staining with 7-amino-actinomycin D (BD Biosciences, Heidelberg, Germany). FACS sorting was performed on a FACSAria cell-sorting system (BD Biosciences, Heidelberg, Germany).

**Cytokine analysis.** A total of $2 \times 10^5$ purified CD11c$^{+}$ DCs were cultivated in 200 μl RPMI 1640 supplemented with 25 mM HEPES, 2 mM L-glutamine (all from Invitrogen, Karlsruhe, Germany), 10% fetal calf serum (Perbio, Bonn, Germany), 50 U/ml penicillin, 50 μg/ml streptomycin (all from Lonza, Verviers, Belgium), and 50 μM β-mercaptoethanol in a 96-well plate at 37°C for 24 h. As a positive control for cytokine secretion, 1 μg/ml R848 (TLR7/8 agonist) or 10 μg/ml CpG DNA 1826 (TLR9 agonist) was added to $2 \times 10^5$ CD11c$^{+}$ DCs. After 24 h, the supernatant was removed and frozen until used. Adherent DCs were lysed in 100 μl TriFast (peqlab, Erlangen, Germany) to isolate RNA for quantitative reverse transcription-PCR (qRT-PCR) as described below. The supernatant was analyzed using a multiplex immunoassay kit (Linco, St. Charles, MO) according to the manufacturer's recommendations. The following cytokines were analyzed using a Luminex 100 IS system (Luminex, Austin, TX): interleukin-1β (IL-1β), IL-2, IL-4, IL-6, IL-7, IL-10, IL-12p70, IL-15, TNF-α, IFN-γ, granulocyte-macrophage colony-stimulating factor (GM-CSF), macrophage inflammatory protein 1α, monocyte chemoattractant protein 1, RANTES, and interferon-inducible protein 10 (IP-10).

**Generation of bone marrow-derived DCs (BMDCs).** Mouse immature DCs were generated from bone marrow according to standard protocols (20). Minor modifications included a full replacement of culture medium containing GM-CSF (200 U/ml) on day 2 (removal of nonadherent cells), whereas on day 4 about 75% of medium with GM-CSF (200 U/ml) was replaced. Iscove's modified Dulbecco's medium supplemented with 5% FCS (Perbio, Bonn, Germany), L-glutamine, and Na-pyruvate (both from Invitrogen, Karlsruhe, Germany) was used as culture medium. On day 6, immature DCs were infected for 1 h with a multiplicity of infection of 10 of purified CVB3 and subsequently washed and incubated for an additional 2 to 23 h in order to allow viral entry and replication.

**IFN-γ secretion of splenocytes.** Isolated splenocytes from mice either uninfected or CVB3 infected 8 days earlier were restimulated with viral antigen preparation for 4 days, and culture supernatants were screened for cytokine production by a sandwich enzyme-linked immunosorbent assay using an OptEIA kit (BD Biosciences, Heidelberg, Germany) according to the manufacturer's instructions, with the modification that 50-μl aliquots of the supernatants were incubated overnight at 4°C.

**PCR and qRT-PCR.** Cells were lysed in TriFast (peqlab, Erlangen, Germany) according to the manufacturer's instructions. RNA (500 ng) was used for reverse transcription using a one-step RT-PCR kit (Qiagen, Hilden, Germany). Real-time qRT-PCR was performed with appropriate annealing temperatures for 40 cycles. The primers were purchased from MWG Biotech (Ebersberg, Germany) and are listed in Table 1.

**Electron microscopy.** For electron microscopy, BMDCs were infected with a multiplicity of infection of 10 of purified CVB3 for 0, 1, 3, 12, and 24 h, washed three times with medium, fixed for 4 h in 2.5% glutaraldehyde (Paesel and Lorei, Hanau, Germany) in 0.1 M cacodylate buffer (pH 7.4), scraped from the substrate, and pelleted. In addition, DCs isolated from mice obtained at different days postinfection were collected and centrifuged to create a pellet. The pellets were washed in cacodylate buffer, postfixed overnight in 1% $OsO_4$ in cacodylate buffer for 1 h, dehydrated in an ascending series of ethanol and propylene oxide, bloc stained in uranyl acetate for 4 h, and flat embedded in Araldite (Serva, Germany). Using an ultramicrotome (Ultracut, Leica, Bensheim, Germany), semithin (1-μm) and ultrathin (50-nm) sections were cut. Ultrathin sections were stained with lead citrate, mounted on copper grids, and finally analyzed with a Zeiss EM 10 electron microscope (Oberkochen, Germany).

**Cytospin preparations.** A total of $1 \times 10^5$ purified DCs in a total volume of 100 μl were applied to cytospin wells and centrifuged at 400 rpm for 5 min. The adherence of the cells on the sialinylized slides was checked, and the slides were air dried for at least 30 min. Then, slides were fixed in 4% buffered paraformaldehyde for 15 min at 4°C, washed twice in distilled water, and subsequently dehydrated in graded ethanol solutions (70% to 95%) and further processed for in situ hybridization.

**Histology.** Hearts were fixed in 4% buffered paraformaldehyde for 12 h at 4°C. After embedding in paraffin, hearts were cut in 5-μm-thick sections and stained with hematoxylin and eosin (H&E) to assess myocardial injury and inflammation as previously described (43).

**In situ hybridization.** Paraffin-embedded heart sections were dewaxed and hybridized with a $^{35}$S-labeled RNA probe specific for genomic plus- and minus-strand CVB3 RNA as described elsewhere (25). CVB3-specific probes were synthesized from the dual-promoter plasmid pCVB3-R1. Control RNA probes were obtained from the vector pSPT18. Slide preparations were subjected to autoradiography, exposed for 3 weeks at 4°C, and counterstained with H&E.

**Statistical analysis.** All data are expressed as means, and errors are displayed as standard errors of the means. All samples were unpaired, and differences between groups were analyzed by an unpaired Student *t* test or by a Mann-Whitney rank sum test. A difference between two groups was judged to be significant if $P$ was $<0.05$.

## RESULTS

**$T_h$2 bias of A.BY/SnJ compared to C57BL/6 mice, but with no major differences revealed in the immune cell repertoire.** In initial experiments the composition of the immune system was assessed in permissive A.BY/SnJ and resistant C57BL/6 mice in the course of CVB3 infection. At various time points postinfection splenocytes were isolated and analyzed by flow cytom-

TABLE 1. Primers used in the study

| Target gene | Orientation | Sequence[a] |
|---|---|---|
| HPRT | F | 5′-TTT GCC GCG AGC CG-3′ |
| | R | 5′-TAA CCT GGT TCA TCA TCG CTA ATC-3′ |
| | Probe | 5′-FAM-CGA CCC GCA GTC CCA GCG TC-TAMRA-3′ |
| IP-10 | F | 5′-GCC GTC ATT TTC TGC CTC AT-3′ |
| | R | 5′-GCT TCC CTA TGG CCC TCA TT-3′ |
| | Probe | 5′-FAM-TCT CGC AAG GAC GGT CCG CTG-TAMRA-3′ |
| Pan enterovirus | F | 5′-TCC TCC GGC CCC TGA-3′ |
| | R | 5′-RAT TGT CAC CAT AAG CAG CCA-3′ |
| | Probe | 5′-FAM-CGG AAC CGA CTA CTT TGG GTG WCC GT-TAMRA-3′ |
| IFN-α | F | 5′-CTT CCA CAG GAT CAC TGT GTA CCT-3′ |
| | R | 5′-TTC TGC TCT GAC CAC CTC CC-3′ |
| | Probe | 5′-FAM-AGA GAG AAG AAA CAC AGC CCC TGT GCC-TAMRA-3′ |
| IFN-β | F | 5′-CTG GAG CAG CTG AAT GGA AAG-3′ |
| | R | 5′-CTT CTC CGT CAT CTC CAT AGG G-3′ |
| | Probe | 5′-FAM-CAA CCT CAC CTA CAG GGC GGA CTT CAA G-TAMRA-3′ |
| TLR3 | F | 5′-CGA AAG TTG GAC TTG TCA TCA AAT-3′ |
| | R | 5′-ACT TGC CAA TTG TCT GGA AAC AC-3′ |
| | Probe | 5′-FAM-CAC TTA AAG AGT TCT CCC-TAMRA-3′ |
| CVB3 | F | 5′-CGG TAC CTT TGT GCG CCT GT-3′[b] |
| | R | 5′-GTT CCG CTG CAG AGT TGC CCG-3′[b] |
| CVB3 nested | F | 5′-CCC CGG ACT GAG TAT CAA TA-3′ |
| | R | 5′-CAG TTA GGA TTA GCC GCA TT-3′ |
| HPRT | F | 5′-GAC AAC AGC CTC AAG ATC ATC-3′[b] |
| | R | 5′-GAC GGC AGG TCA GGT CCA CCA-3′[b] |
| HPRT nested | F | 5′-AAT GCC TCC TGC ACC ACC-3′ |
| | R | 5′-ATG CCA GTG AGC TTC CCG-3′ |

[a] FAM, 6-carboxyfluorescein; TAMRA, 6-carboxytetramethylrhodamine.
[b] Primers used for cDNA synthesis.

etry (Fig. 1A). In comparison to C57BL/6 mice, A.BY/SnJ mice showed significantly higher levels of $CD4^+$ T cells ($CD3^+$ $CD4^+$) at days 4, 8, and 12 postinfection (p.i.), whereas $CD8^+$ T cells ($CD3^+$ $CD8^+$) were reduced in the course of infection, which is indicative for a $T_h2$ bias of A.BY/SnJ mice. Sustaining the $T_h2$ bias of A.BY/SnJ mice, IFN-γ secretion was reduced in in vitro-stimulated splenocytes derived from A.BY/SnJ mice, as we demonstrated previously (43). Moreover, in A.BY/SnJ mice the increase of $CD8^+$ T cells was delayed during acute infection (8 days p.i.), and the amount of this cell population was significantly decreased compared to C57BL/6 mice. The comparison of B cells revealed consistently lower amounts of B cells in permissive mice than in resistant animals at any time of infection. However, as we have shown previously, these discrepancies were not reflected by differences in the titers of CVB3-specific immunoglobulin G and neutralizing antibodies (43).

In comparing uninfected A.BY/SnJ and C57BL/6 mice, slightly increased levels of monocytes ($CD11b^+$) and NK cells ($Dx5^+$ $CD3^-$) were measured. However, in the course of infection the differences between the two mouse strains were no longer apparent. No significant differences were noted for regulatory T cells ($CD4^+$, $CD25^+$, $FoxP3^{high}$). Furthermore, the patterns of the relative amounts of NK cells, monocytes, and regulatory T cells during infection were rather similar in A.BY/SnJ and C57BL/6 mice.

**Differences in DC subpopulations from A.BY/SnJ and C57BL/6 mice.** In addition to the leukocyte analysis, the levels of pDCs ($mPDCA^+$) and DCs ($CD11c^+$) were assessed by flow cytometry (Fig. 1B) in the two mouse strains. In A.BY/SnJ mice, the increase of pDCs was about twice as high as in C57BL/6 mice at days 4 and 8 p.i. The kinetics of pDC expansion was similar in both mouse strains, peaking at day 4 p.i. $CD11c^+$ DCs, however, showed an earlier and significantly higher response to CVB3 infection in C57BL/6 mice. At day 8 p.i. and later, the relative amounts of DCs had reached equal levels in A.BY/SnJ and C57BL/6 mice.

Further analysis of DC subpopulations of A.BY/SnJ mice revealed significantly increased levels of myeloid $CD4^+/CD8^-$ DCs, which are known to be $CD4^+$ T-cell activating (37) and potent in cytokine production (38) (Fig. 1C). $CD4^-$ $CD8^+$ DCs, which are most competent in cross-presentation to $CD8^+$ T cells (11, 40), as well as $CD4^-$ $CD8^-$ DCs, were present in C57BL/6 mice in higher amounts than in A.BY/SnJ mice. At any time of infection, the ratio of $CD4^-$ $CD8^+$ DCs to $CD4^+$ $CD8^-$ DCs was significantly higher in C57BL/6 mice, reaching its maximum at day 8 p.i.

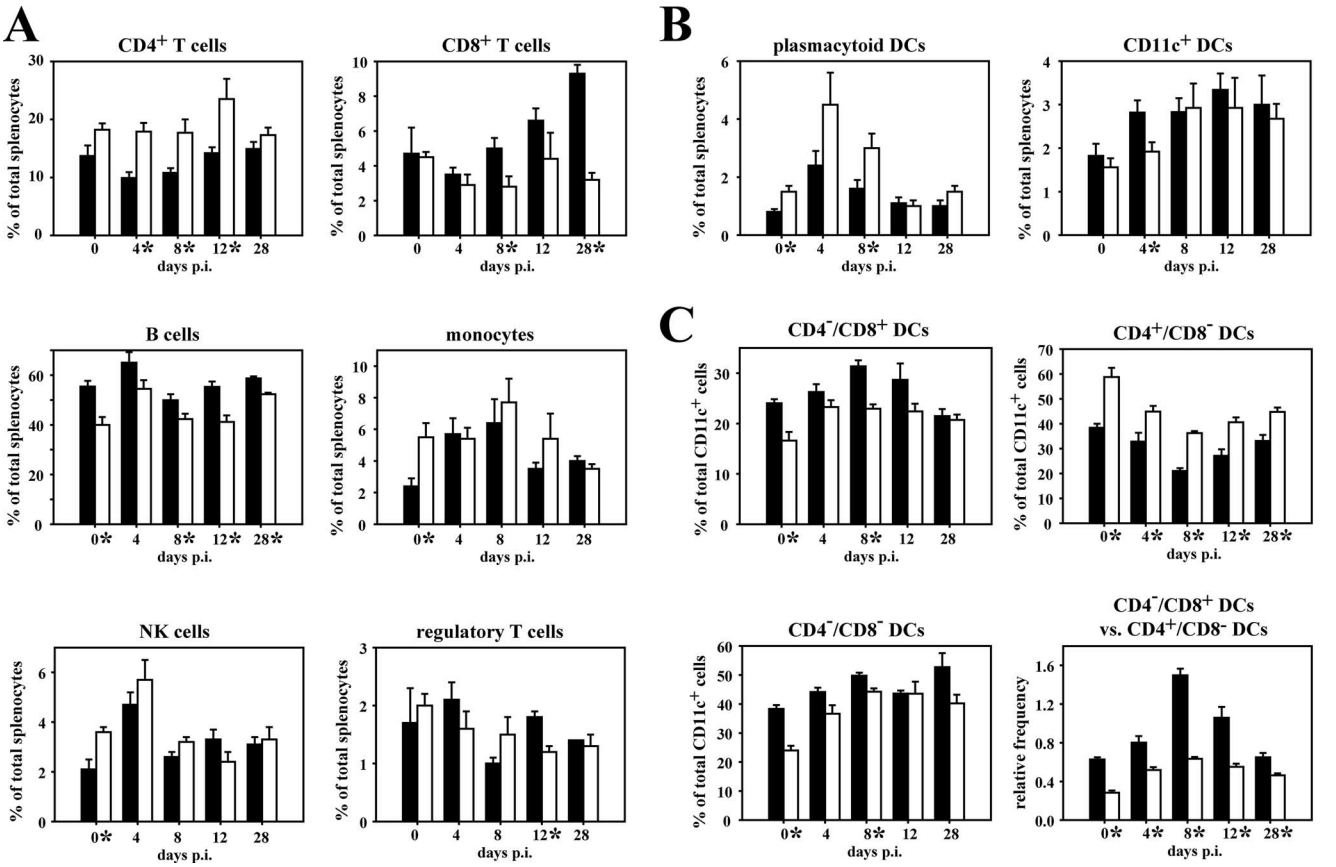


FIG. 1. Analysis of immune cell subsets of A.BY/SnJ and C57BL/6 mice by flow cytometry. A) FACS analysis of splenocytes isolated from A.BY/SnJ mice (white bars) and C57BL/6 mice (black bars) at various time points post-CVB3 infection (six mice per bar). B) A corresponding analysis was performed for pDCs and CD11c$^+$ DCs (7 to 10 mice per bar). C) Subtype distribution of CD11c$^+$ DCs in the course of CVB3 infection (7 to 10 mice per bar). All error bars represent standard errors of the means; significant differences are marked with an asterisk on the indicated day.

**CVB3 can infect BMDCs in vitro.** For a detailed analysis regarding the interaction of CVB3 and DCs early in CVB3 infection, we generated bone marrow-derived DCs and infected them with CVB3. Mock-infected BMDCs were used as a negative control (data not shown). Electron microscopy (Fig. 2A) obtained at 1 h p.i. revealed the attachment of a virus particle to the cell surface and its uptake in a clathrin-coated pit (left image). At 3 h p.i. virus particles are present in early endosomes (right image), a finding which was recently described in CVB3-infected HeLa cells (9). The overview of the CVB3-infected BMDCs (bottom) reveals typical vesiculated areas, which are indicative of enterovirus replication processes (15). Further evidence for CVB3 replication in BMDCs was assessed by the detection of replicative minus-strand RNA intermediates as detected by specific RT-PCR from cells obtained 3 h and 24 h p.i. (Fig. 2B). The results obtained in infected BMDCs were comparable in both mouse strains. Importantly, no infectious virus particles were generated in infected BMDCs at any time postinfection, as determined by plaque assays (data not shown).

**CVB3 infects pDCs and DCs in vivo, but replication is restricted.** To determine whether DCs and pDCs are also infected in vivo we performed RT-PCR for the differential detection of viral plus- and replicative minus-strand RNA. Plus-strand CVB3 RNA molecules were detected in DCs obtained at days 4 and 8 p.i. and in FACS-sorted pDCs, respectively (Fig. 2B; purity, >99%). Also, minus-strand CVB3 RNA was detected in DCs and pDCs of both mouse strains. In C57BL/6 mice only plus-strand RNA but no minus-strand CVB3 RNA was detectable in DCs at day 8 p.i. These observations were confirmed by in situ hybridization experiments. As illustrated in Fig. 2C, DCs from C57BL/6 mice obtained at day 4 p.i. revealed replicative minus-strand CVB3 RNA intermediates in lower copy numbers than genomic CVB3 RNA molecules, as reflected in the different number of silver grains in autoradiographs. No infectious virus progeny was isolated from infected DCs or pDCs at any time after infection, indicating the lack of complete replication cycles.

In comparing CVB3 RNA isolated from DCs from day 4 and day 8 p.i. in the two mouse strains by quantitative RT-PCR, we found that the load of viral RNA in DCs isolated from A.BY/SnJ mice was 3- to 10-fold higher than in DCs derived from C57BL/6 mice (Fig. 2D). No CVB3 RNA was detectable in DCs isolated on day 28 p.i. of both mouse strains.

**CVB3-induced expression of IFN-α and IFN-β by pDCs is reduced in A.BY/SnJ mice compared to C57BL/6 mice.** In further experiments we investigated whether functional differences of pDCs and DCs are determinants for the different

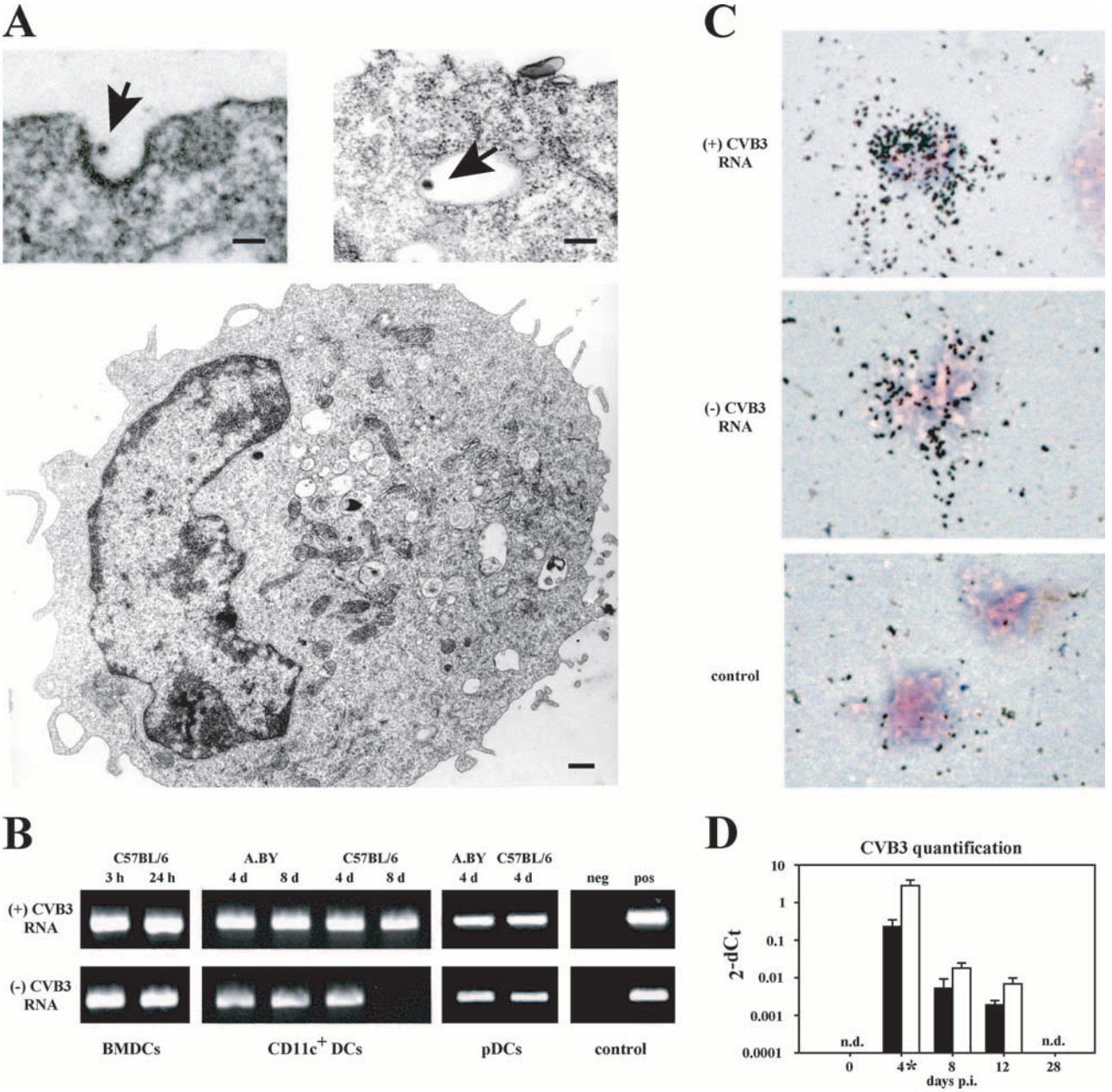


FIG. 2. CVB3 can infect DCs in vitro and in vivo, but replication is impaired. A) Electron microscopy of BMDCs infected in vitro with CVB3. The upper left panel shows viral attachment at the cell surface and its uptake in a clathrin-coated pit (arrow); the right panel demonstrates that CVB3 is taken up in endosomes (arrow). Bar, 75 nm. The bottom panel shows an infected BMDC 24 h p.i. Bar, 1 μm. B) Strand-specific RT-PCR analysis of DC subtypes from C57BL/6 and A.BY/SnJ mice revealed that all analyzed DC subtypes are positive for genomic plus-strand (+) CVB3 RNA after infection. Replicative minus-strand (−) CVB3 RNA intermediates were also found in all DCs, except in $CD11c^+$ DCs isolated from C57BL/6 at 8 days p.i. C) In situ hybridization of $CD11c^+$ DCs isolated from C57BL/6 at day 4 p.i. showed quantitatively higher amounts of genomic plus-strand (+) CVB3 RNA compared to minus-strand (−) CVB3 RNA. Negative controls were derived from uninfected murine spleens and positive controls were from acutely CVB3-infected murine spleens as published previously (27). D) Quantification of CVB3 genomes by qRT-PCR in $CD11c^+$ DCs. A.BY/SnJ mice (white bars) showed higher viral loads than C57BL/6 mice (black bars) ($n = 6$). Data from panels B and C are representative of at least three independent experiments. Error bars represent standard errors of the means. Significant differences are marked with an asterisk at the indicated day.

courses of infection in the two mouse strains. As pDCs are most potent in producing type I interferons upon viral infection (10), we analyzed IFN-α and -β mRNA levels in pDCs isolated from A.BY/SnJ mice and C57BL/6 mice 4 days p.i., when the pDC frequency reached a maximum in both mouse strains. pDCs were isolated by magnetic-activated cell sorting from spleens, and interferon levels were analyzed by qRT-PCR (Fig. 3). As the purity of isolated pDCs was only >60%, mPDCA-negative splenocytes served as a control to exclude IFN detection due to any contaminating cells. pDCs derived from

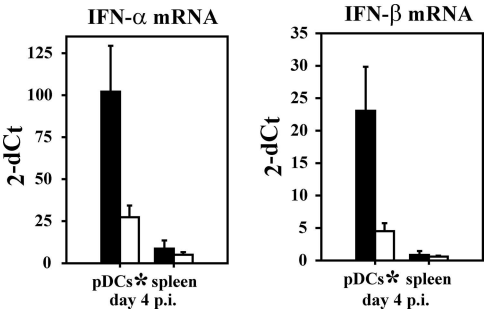


FIG. 3. Interferon type I expression in pDCs isolated from A.BY/SnJ and C57BL/6 mice 4 days post-CVB3 infection. Quantitative RT-PCR analysis of pDCs isolated from A.BY/SnJ (white bars) and C57BL/6 (black bars) mice revealed significantly increased IFN-α and IFN-β levels in C57BL/6 mice. To exclude interferon secretion due to contaminating cells, non-pDC splenocytes were additionally tested for interferon secretion. $n = 7$ per bar, and error bars represent standard errors of the means. Significant differences are marked with an asterisk on the legend of the $x$ axis.

C57BL/6 mice were found to express approximately four times higher magnitudes of both IFN-α and IFN-β ($P < 0.05$). These findings were confirmed in FACS-sorted pDCs of both mouse strains. However, differences in the total amount of secreted IFNs were relative, as A.BY/SnJ mice exhibited increased pDC levels at day 4 p.i. (Fig. 1B).

**Delayed secretion of proinflammatory cytokines derived from DCs of A.BY/SnJ mice upon CVB3 infection.** To investigate whether DCs from C57BL/6 and A.BY/SnJ mice vary in their repertoires of cytokine production, DCs were isolated from spleens at various time points post-CVB3 infection and cultivated for 24 h. The supernatants were analyzed by multiplex immunoassays to assess their levels of various secreted cytokines. As positive controls, cells were stimulated with the TLR7/8 or TLR9 agonists R848 or CpG DNA, respectively, and exhibited similar levels of cytokine secretion at different times after infection; thus, they were combined as "stimulated." IL-1β, IL-4, IL-7, IL-15, IFN-γ, and GM-CSF were not detected in any of the supernatants in significant amounts, and IL-2, IL-12p70, and monocyte chemoattractant protein 1 were only present in the stimulated samples (data not shown). Here, a significant difference between both mouse strains was only observable for IL-2, which was reduced in samples derived from A.BY/SnJ mice at any time of infection.

Moreover, cytokine analysis revealed that DCs isolated from A.BY/SnJ and C57BL/6 mice are capable of secreting the proinflammatory cytokines IL-6 and TNF-α (Fig. 4). The maximal release of IL-6 as well as of TNF-α was found at day 8 p.i. in C57BL/6 mice, whereas A.BY/SnJ mice reached the maximal release of these proinflammatory cytokines only at day 12 p.i. In both mouse strains, the cytokine levels induced by CVB3 infection in vivo were only about 10% of the maximal release as observed by in vitro stimulation with TLR agonists.

Interestingly, IL-10 secretion was significantly increased in DCs isolated from C57BL/6 mice at any time postinfection. At day 8 p.i., secretion was elevated 4.5-fold compared to DCs of corresponding A.BY/SnJ mice. In infected A.BY/SnJ mice, however, there was no increase in IL-10 secretion over time.

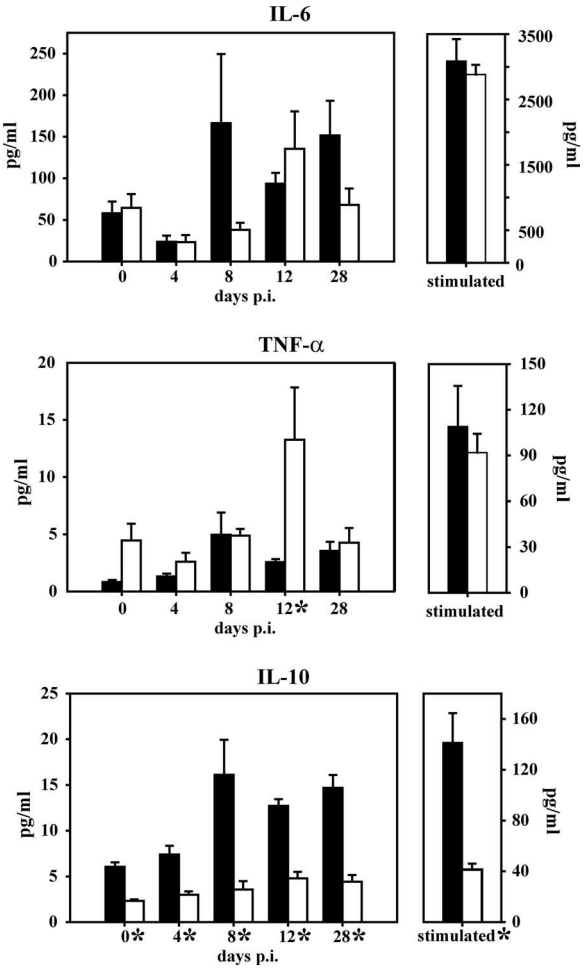


FIG. 4. Delayed secretion of cytokines by DCs isolated from A.BY/SnJ and C57BL/6 mice at various time points post-CVB3 infection. Multiplex immunoassay analysis of cytokines secreted by $CD11c^+$ DCs isolated from C57BL/6 (black bars) and A.BY/SnJ (white bars) mice after 24-h in vitro cultivation. DCs of different mouse strains varied in their cytokine secretion patterns and in the absolute amount of secreted cytokines. As positive controls, cells were stimulated with the TLR7/8 or TLR9 agonists R848 or CpG DNA, respectively, exhibiting similar levels of cytokine secretion during infection and were thus combined as "stimulated." $n = 3$ per bar, and error bars represent standard errors of the means. Significant differences are marked with an asterisk on the legend of the $x$ axis.

**Differential chemokine secretion by DCs of CVB3-infected A.BY/SnJ and C57BL/6 mice.** Among all parameters analyzed by multiplex immunoassay, the lymphocyte attractant chemokines IP-10 and RANTES were most prominent with regard to absolute amounts in DCs (Fig. 5A). Importantly, in comparison to RANTES, IP-10 was expressed at a 50-fold higher level and was the only parameter for which in vitro stimulation did not lead to a further increase of secretion. In DCs of C57BL/6 mice, IP-10 and RANTES were secreted earlier and for a sustained period, and even at 28 days p.i. high levels of IP-10 and RANTES were detectable, in contrast to DCs of A.BY/SnJ mice. The kinetics of IP-10 and RANTES secretion were verified at the mRNA level by qRT-PCR (Fig. 5B). FACS analyses for the expression of the receptors for RANTES (CCR5)

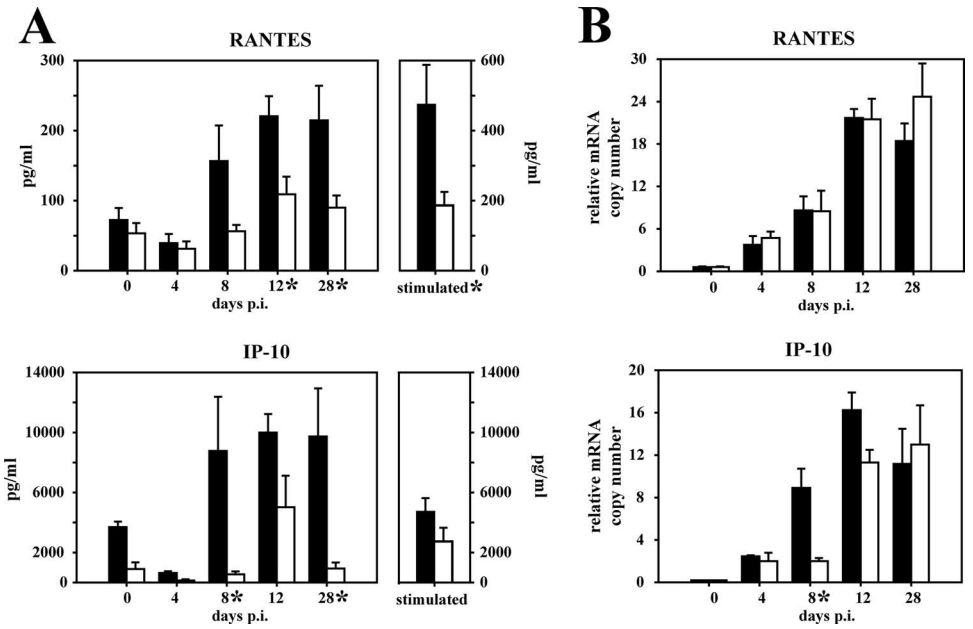


FIG. 5. Differential secretion of the T-cell-attractive chemokines IP-10 and RANTES by DCs isolated from C57BL/6 and A.BY/SnJ mice at different times post-CVB3 infection. As positive controls, cells were stimulated with the TLR7/8 or TLR9 agonists R848 or CpG DNA, respectively, and exhibited similar levels of cytokine secretion at different time points of infection, and thus they were combined as "stimulated." $CD11c^+$ DCs isolated from C57BL/6 (black bars) and A.BY/SnJ (white bars) mice were cultured for 24 h in vitro. A) Supernatants were tested by multiplex immunoassay and revealed an earlier and more pronounced IP-10 and RANTES secretion in C57BL/6-derived DCs. B) RNA was isolated from the same samples as described above. Expression levels of RANTES and IP-10 were analyzed by qRT-PCR. All error bars represent standard errors of the means ($n = 3$). Significant differences are marked with an asterisk on the respective day.

and IP-10 (CXCR3) on T cells of A.BY/SnJ and C57BL/6 mice were not quantitatively different (data not shown).

**$IP\text{-}10^{-/-}$ mice show enhanced myocardial damage but no virus persistence.** Among all analyzed chemokines and cytokines, IP-10 was secreted in DCs in the highest quantities, and its secretion patterns revealed the most distinct differences between C57BL/6 and A.BY/SnJ mice in the course of CVB3 infection. The relevance of this chemokine in CVB3 myocarditis is substantiated by the finding of a strong IP-10 expression in inflammatory mononuclear cells within myocardial lesions of acutely infected C57BL/6 mice (Fig. 6A). As exemplarily shown in a C57BL/6 mouse heart obtained at day 4 p.i., this chemokine appears to be involved in the early T-cell invasion into the infected heart, which is known to be necessary for efficient virus elimination. In contrast, $IP\text{-}10^{-/-}$ mice revealed obviously less attraction of $CD3^+$ T cells in CVB3-infected hearts at day 4 p.i. (Fig. 6B). In order to further analyze the role of IP-10 secretion for the development of chronic myocarditis in vivo, we investigated $IP\text{-}10^{-/-}$ mice phenotypically and functionally following CVB3 infection. In comparison to resistant C57BL/6 mice, $IP\text{-}10^{-/-}$ mice showed extensive cardiac lesions during acute infection (Fig. 6C, H&E staining). Interestingly, viral loads were similar to those of C57BL/6 mice as shown by in situ hybridization (Fig. 6C, ISH). Low viral titers during acute infection were found to be correlated with a pronounced IFN-γ secretion of in vitro-stimulated splenocytes (Fig. 6D), which was even higher than in C57BL/6 mice. $IP\text{-}10^{-/-}$ mice showed reduced levels of T-cell infiltration early in CVB3 infection compared to C57BL/6 mice (Fig. 6B). However, correspondent to C57BL/6 mice, $IP\text{-}10^{-/-}$ mice were also found to be capable of eliminating the virus during acute infection, and thus no chronic myocarditis developed in these animals.

**TLR3 is crucial for the control of CVB3 infection.** As described above, C57BL/6 mice carried significantly higher levels of cross-priming $CD4^-$ $CD8^+$ DCs than A.BY/SnJ mice (Fig. 1C). In this cell population, TLR3 was found to be expressed in about 10-fold higher amounts compared to other DC subtypes and pDCs (data not shown) (14). Therefore, we focused on TLR3-mediated recognition of CVB3 and its role as molecular sensor of CVB3 myocarditis by investigating $TLR3^{-/-}$ mice.

Histology of hearts from $TLR3^{-/-}$ mice obtained 8 days p.i. showed severe inflammatory lesions and viral loads which were even more pronounced than in permissive A.BY/SnJ mice (Fig. 6C). In line with our observations in A.BY/SnJ mice, no significant increase in IFN-γ secretion of in vitro-stimulated $TLR3^{-/-}$ splenocytes was detectable upon CVB3 infection. In order to assess the functionality of pDCs and DCs in $TLR3^{-/-}$ mice as far as their potential to secrete key cytokines and chemokines is concerned, we isolated DCs (8 days p.i.) and pDCs (4 days p.i.) from the spleens of these animals. IFN-α and IFN-β expression levels of pDCs were analyzed by qRT-PCR (Fig. 7). pDCs from $TLR3^{-/-}$ mice had significantly reduced expression levels of both type I interferons compared to C57BL/6 mice. IFN-β expression of DCs derived from $TLR3^{-/-}$ mice was also significantly reduced compared to A.BY/SnJ mice. Moreover, the expression of RANTES and IP-10 was analyzed in DCs derived from infected $TLR3^{-/-}$

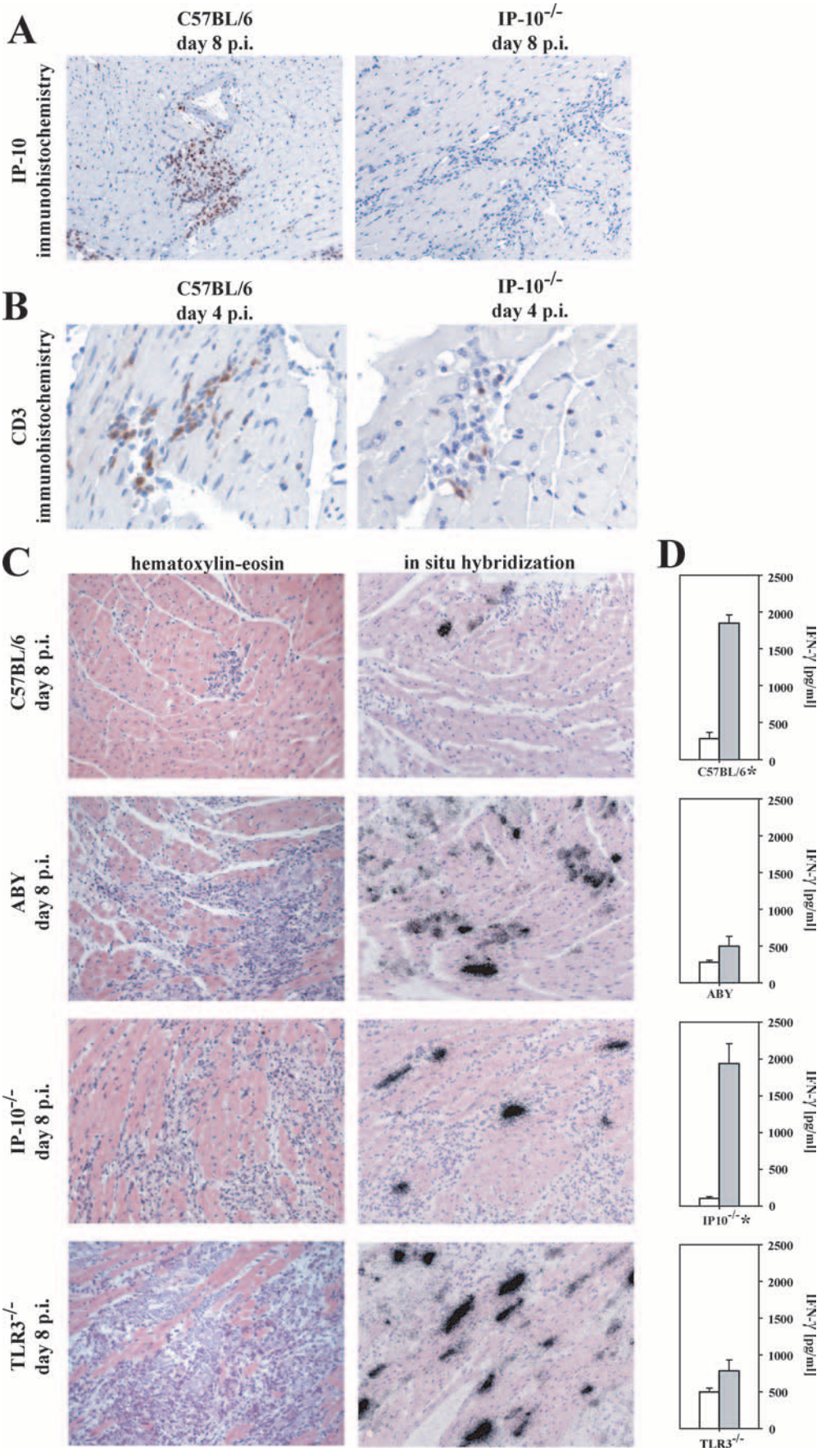
A
C57BL/6
day 8 p.i.
IP-10$^{-/-}$
day 8 p.i.
IP-10
immunohistochemistry
B
C57BL/6
day 4 p.i.
IP-10$^{-/-}$
day 4 p.i.
CD3
immunohistochemistry
C
hematoxylin-eosin
in situ hybridization
C57BL/6
day 8 p.i.
ABY
day 8 p.i.
IP-10$^{-/-}$
day 8 p.i.
TLR3$^{-/-}$
day 8 p.i.
D
IFN-γ [pg/ml]
2500
2000
1500
1000
500
0
C57BL/6*
ABY
IP10$^{-/-}$*
TLR3$^{-/-}$

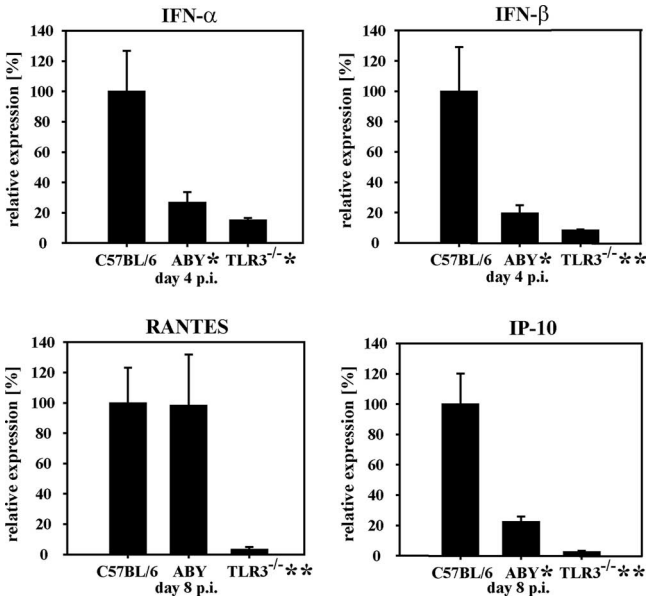


FIG. 7. DCs of TLR3$^{-/-}$ mice were defective in cytokine and chemokine expression. Results are shown for the qRT-PCR analysis of type I interferon expression in pDCs and of RANTES and IP-10 in CD11c$^{+}$ DCs, respectively. All expression levels of resistant C57BL/6 mice were defined as 100% expression. All error bars represent standard errors of the means ($n = 5$). *, significant difference in TLR3$^{-/-}$ mice versus C57BL/6 mice; **, significant difference in TLR3$^{-/-}$ mice versus C57BL/6 mice and A.BY/SnJ mice.

mice with the result that the expression of both cytokines was abrogated almost entirely.

## DISCUSSION

In previous studies we have shown that resistance to the development of chronic CVB3 myocarditis in mice is dependent on CD8$^{+}$ T cells expressing cardioprotective cytokines, such as IFN-γ (26). CVB3 infection of A.BY/SnJ mice (*H-2$^{b}$*) and C57BL/6 mice (*H-2$^{b}$*) was found to result in a completely different course of infection. In A.BY/SnJ mice, infection with CVB3 leads to an ongoing, chronic form of myocarditis which is based on virus persistence, whereas C57BL/6 mice suffer only from acute infection because they are able to clear the virus during the acute phase of infection (25). As A.BY/SnJ and C57BL/6 mice express the same MHC antigens, their CD8$^{+}$ T cells are supposed to recognize identical viral epitopes. Thus, it is unlikely that the differences in the course of infection are caused by a fundamental inability of T cells derived from A.BY/SnJ mice to recognize dominant *H-2$^{b}$*-restricted CVB3 epitopes. However, we observed a delayed and less pronounced CD8$^{+}$ T-cell expansion in permissive A.BY/SnJ mice, substantiating our previous observations that these cells are protective in CVB3 myocarditis (26). To identify immune parameters which might explain these differences in T-cell expansion, we analyzed further immune cell subsets in these two mouse strains. A.BY/SnJ mice revealed a T$_h$2-biased phenotype with increased levels of CD4$^{+}$ T cells and a lack of IFN-γ production upon in vitro stimulation of splenocytes with heat-inactivated CVB3. This could favor an antibody-mediated immune response rather than a cellular one. However, as previously demonstrated, there were no significant differences in the titers of CVB3-specific immunoglobulin G and neutralizing antibodies in A.BY/SnJ mice and C57BL/6 mice (43); thus, the humoral immune response seems not to be the major factor in the regulation of the outcome of myocarditis.

Regulatory T cells are potent inhibitors of T-cell effector function (6). Thus, the lack of a sufficient antiviral immune response and CD8$^{+}$ T-cell expansion in A.BY/SnJ mice might have been caused by changes in regulatory T cells. Yet, there was neither a difference in regulatory T-cell frequency (CD4$^{+}$, CD25$^{+}$, FoxP3$^{high}$) between uninfected A.BY/SnJ and C57BL/6 mice nor a change in their frequency in the course of CVB3 infection. On the other hand, the limited expansion of CD8$^{+}$ T cells in A.BY/SnJ mice during CVB3 infection might reflect a deficit in T-cell activation. DCs belong to the most potent antigen-presenting cells, and with a DC stimulus, T-cell proliferation can efficiently be induced (41). Thus, we analyzed the frequency, subtype distribution, and functionality of DCs in A.BY/SnJ and C57BL/6 mice in the course of CVB3 infection. Importantly, we found a delayed response of CD11c$^{+}$ DC expansion as well as decreased levels of cross-priming CD4$^{-}$ CD8$^{+}$ DCs in A.BY/SnJ mice. CD4$^{-}$ CD8$^{+}$ DCs, which have been shown to be most potent in MHC-I-dependent activation of CD8$^{+}$ T cells (37) are known to be T$_h$1 directing (31). Thus, we suggest that the lack of CD4$^{-}$ CD8$^{+}$ DCs in A.BY/SnJ mice may contribute to their inability to limit CVB3 infection early in disease.

In subsequent experiments we considered whether DC function might be impaired in CVB3 infection, interfering with an adequate CD8$^{+}$ T-cell activation. Both in vitro and in vivo experiments showed that DCs can be infected by CVB3 but that complete viral replication was impaired and no infectious virus progeny could be isolated from DCs. Restricted viral replication in DCs has also been reported for other RNA viruses, such as SARS coronavirus (28) or the foot-and-mouth disease virus (36). Yet, this impaired replication in DCs is not a general phenomenon of RNA viruses. Indeed, it was shown for Ebola, Marburg, and Lassa viruses that DCs can also be productively infected (4, 7). Why viral replication is inhibited although replicative minus-strand RNA intermediates are gen-

FIG. 6. Susceptibility of IP-10$^{-/-}$ mice and TLR3$^{-/-}$ mice to CVB3 infection. A) IP-10 expression in cardiac immune cells of CVB3-infected C57BL/6 mice was demonstrated by immunohistochemistry. As expected, control staining of IP-10$^{-/-}$ mouse hearts was negative. Magnification, ×80. B) Immunohistochemical labeling of CD3$^{+}$ T cells early in infection (4 days p.i.) demonstrated that in cardiac lesions of resistant C57BL/6 mice more T cells are present than in those of IP-10 knockout mice. Magnification, ×200. C) Hearts of CVB3-infected mice of various strains were analyzed by histology and in situ hybridization and showed various extents of myocardial damage and infection. Magnification, ×80. D) Splenocytes of uninfected mice (white bars) and of mice which were infected with CVB3 for 8 days (gray bars) were stimulated in vitro for 4 days with heat-inactivated CVB3. Supernatants were analyzed by enzyme-linked immunosorbent assay for IFN-γ secretion. Significant differences are marked with an asterisk; all error bars represent standard errors of the means ($n \geq 3$).

erated in DCs is not known for SARS coronavirus or for CVB3. However, the presence of viral RNA in DCs can lead to DC activation mediated by TLR7/8 (12) or TLR3 (40). In comparing DC activation markers such as MHC-II, CD80, or CD86, no significant differences were found between A.BY/SnJ and C57BL/6 in the course of CVB3 infection (data not shown). However, we observed a divergent production of cytokines and chemokines in DCs following CVB3 infection in these mouse strains.

Similar to the SARS coronavirus model, we found an induction of proinflammatory cytokines in CVB3-infected mice albeit with rather low levels of IL-6 and TNF-α secretion by splenic DCs at various times postinfection. Interestingly, significant differences between A.BY/SnJ mice and C57BL/6 mice were observed in IL-10 production. IL-10, which is highly expressed in DCs isolated from resistant C57BL/6 mice, was shown to be cardioprotective, because exuberant immune reactions were restricted and thus excessive inflammation (23, 43) was avoided. Therefore, myocardial damage at later stages of infection in A.BY/SnJ mice as a result of ongoing inflammation might be exacerbated by the lack of IL-10. Furthermore, IL-10 and RANTES protein secretion levels of in vitro-stimulated DCs differed significantly in A.BY/SnJ and C57BL/6 mice. These findings point to MHC-independent inherent differences of the DCs from these two mouse strains regarding their ability to respond to CVB3 infection by expressing a divergent repertoire of cytokines and chemokines. In contrast to the rather modest secretion of cytokines in DCs, the chemokines IP-10 and RANTES were induced and secreted by DCs in prominent amounts upon infection with CVB3. Enhanced chemokine expression was also reported for DCs stimulated with TLR ligands (38) or viruses, such as SARS coronavirus (28). Both chemokines are known to be involved in T-cell attraction (13) and expansion (30). In our model system, RANTES and IP-10 were secreted in significantly higher amounts by DCs isolated from resistant C57BL/6 mice compared to permissive A.BY/SnJ mice. Furthermore, sustained IP-10 and RANTES secretion observed in C57BL/6 mice up to day 28 p.i. correlated well with continuously elevated levels of $CD8^+$ T cells in these mice. On the protein level, significant differences in the amounts of IP-10 and RANTES were noted between A.BY/SnJ and C57BL/6 mice. Yet, when comparing the chemokines at the mRNA levels, the differences were less pronounced, especially at day 28 p.i. These differences in protein and mRNA levels might indicate further control of IP-10 and RANTES on a translational level.

As shown in this study, we found considerable expression of IP-10 in immune cells within cardiac lesions in acute CVB3 myocarditis, especially in C57BL/6 mice, which indicates the relevance of this chemokine in T-cell attraction. IP-10 expression has not only been reported in CVB3-infected mouse hearts (48) but also in other inflamed tissues, e.g., after lymphocytic choriomeningitis virus infection of the central nervous system (8). Moreover, it has been described that blocking of IP-10 results in a decrease of antigen-specific T-cell expansion (24), potentially due to the fact that IP-10 secretion is required for the retention of $T_h1$ T cells in lymphoid organs (47). As DCs of infected C57BL/6 mice secreted 50-fold more IP-10 compared to RANTES, we focused in this study on the role of IP-10 in the course of CVB3-mediated myocarditis, although RANTES expression is also reported to be involved in proper T-cell function and expansion (30). Influences of non-DC-mediated events early in infection, e.g., a cytokine milieu shaped by NK cells, are not excluded from our mouse model. However, we have shown for the first time significant MHC-independent differences between A.BY/SnJ and C57BL/6 mice in DC populations which are activated prior to T cells and thus may be of relevance for the different outcomes and courses of infection in susceptible and resistant mouse strains.

In order to analyze the relevance of IP-10 secretion for the course of CVB3-mediated myocarditis in vivo, we determined the phenotype of CVB3-infected IP-$10^{-/-}$ mice. In other virus models, e.g., for dengue virus infection, a significantly higher mortality in IP-$10^{-/-}$ mice was observed (19). In CVB3-infected IP-$10^{-/-}$ mice we found extended cardiac lesions during acute stages of the disease. However, the extent of virus infection in the heart was not as high as typically observed in permissive mice. The efficient clearance of virus from the organism might be partially the result of the pronounced IFN-γ secretion as observed in IP-$10^{-/-}$ splenocytes upon in vitro stimulation with CVB3. Thus, IP-10 expression plays a protective role by limiting cardiac inflammation but is not essential for the potent elimination of CVB3.

In order to obtain further insights into the molecular pathways which are crucial in CVB3-mediated DC activation and in the induction of chemokine and cytokine production in DCs, we followed the course of CVB3 infection in TLR$3^{-/-}$ mice. TLR3, as well as TLR7/8, was reported to induce chemokine and cytokine production in DCs upon contact with RNA viruses (12, 40). In this study, we focused on CVB3 infection of TLR$3^{-/-}$ mice for two reasons. First, in the case of picornavirus infection, cross-priming and thus activation of $CD8^+$ T cells was shown to be largely dependent on TLR3 expression (40). Second, the control of a primary CVB3 infection was found to be independent of intact TLR7/8 signaling (16). After CVB3 inoculation, TLR$3^{-/-}$ mice revealed an almost unrestricted and prolonged replication of CVB3 in the heart. The extents of viral infection and cardiac destruction were even more pronounced than in permissive A.BY/SnJ mice, underlining the relevance of TLR3 in limiting enteroviral replication.

In A.BY/SnJ mice we could verify the findings of Edwards et al. (14) that $CD4^-$ $CD8^+$ DCs, which are most potent in cross-priming, express about 10-fold more TLR3 than other DC subtypes (data not shown). Thus, one possible explanation for the ineffective IFN-γ secretion of in vitro CVB3-stimulated splenocytes isolated from TLR$3^{-/-}$ mice might be a lack of efficient T-cell activation by $CD4^-$ $CD8^+$ DCs in TLR$3^{-/-}$ mice. However, an additional contribution of non-DC-mediated effects of TLR3 in CVB3 infection is well possible. The relevance of an early and efficient IFN-γ secretion in the prevention of chronic myocarditis was shown previously (43). Furthermore, the lack of IFN-γ secretion in TLR$3^{-/-}$ mice might reflect the low levels of IP-10 and RANTES which have been observed in TLR$3^{-/-}$ DCs, as both chemokines are known to be induced by IFN-γ (29). A dependence of RANTES and IP-10 secretion on the presence of TLR3 has also been shown in encephalomyocarditis virus infection (17) and for the respiratory syncytial virus (39). Moreover, the decreased secretion of type I interferons by pDCs may also be attributed to the lack of TLR3, and thus to a lack in TRIF-IRF3 signaling (44). Both

type I interferons, which have been shown to be crucial in CVB3 infection (46), as well as the correct induction of CVB3-specific $CD8^+$ T cells were strongly distorted in $TLR3^{-/-}$ mice, thus determining the inability of $TLR3^{-/-}$ mice to control CVB3 infection.

In summary, resistant C57BL/6 mice are characterized by higher levels of $CD8^+$ T cells and an increased percentage of cross-priming $CD4^-$ $CD8^+$ DCs in the course of CVB3 infection. Furthermore, DCs isolated from C57BL/6 mice secreted the proinflammatory cytokines IL-6 and TNF-α earlier than permissive A.BY/SnJ mice. IL-10 as well as the chemokines IP-10 and RANTES were secreted earlier and in substantially higher amounts in DCs of resistant C57BL/6 mice. $IP\text{-}10^{-/-}$ mice revealed increased myocardial damage but no viral persistence, and ongoing myocarditis was observed, most likely due to the fact that T-cell function of $IP\text{-}10^{-/-}$ mice does not seem to be impaired. Furthermore, we found that TLR3 is crucial for the limitation of CVB3 infection. CVB3 infection of $TLR3^{-/-}$ mice did not induce type I or II interferons in pDCs, and in DCs IP-10 and RANTES secretion was abrogated. CVB3 replication was largely unrestricted in $TLR3^{-/-}$ mice, and this infection resulted in severe ongoing myocarditis with virus persistence. Altogether, our data point to MHC-independent genetic factors qualifying DCs to influence the course of enteroviral myocarditis. However, there are still open questions comprising the identification of these determinants which might be involved in shaping different DC cytokine profiles in susceptible and resistant mice.

## ACKNOWLEDGMENTS

We thank Lynne Yakes for critical reading of the manuscript and Sandra Bundschuh and Carmen Ruoff for excellent technical assistance.

This work was supported by the Deutsche Forschungsgemeinschaft (SFB-TR19 for A.O.W., S.S., and K.K.).

## REFERENCES

1. **Alexopoulou, L., A. C. Holt, R. Medzhitov, and R. A. Flavell.** 2001. Recognition of double-stranded RNA and activation of NF-κB by Toll-like receptor 3. Nature **413:**732–738.
2. **Asselin-Paturel, C., A. Boonstra, M. Dalod, I. Durand, N. Yessaad, C. zutter-Dambuyant, A. Vicari, A. O'Garra, C. Biron, F. Brière, and G. Trinchieri.** 2001. Mouse type I IFN-producing cells are immature APCs with plasmacytoid morphology. Nat. Immunol. **2:**1144–1150.
3. **Baboonian, C., and T. Treasure.** 1997. Meta-analysis of the association of enteroviruses with human heart disease. Heart **78:**539–543.
4. **Baize, S., J. Kaplon, C. Faure, D. Pannetier, M. C. Georges-Courbot, and V. Deubel.** 2004. Lassa virus infection of human dendritic cells and macrophages is productive but fails to activate cells. J. Immunol. **172:**2861–2869.
5. **Banchereau, J., and R. M. Steinman.** 1998. Dendritic cells and the control of immunity. Nature **392:**245–252.
6. **Belkaid, Y.** 2007. Regulatory T cells and infection: a dangerous necessity. Nat. Rev. Immunol. **7:**875–888.
7. **Bosio, C. M., M. J. Aman, C. Grogan, R. Hogan, G. Ruthel, D. Negley, M. Mohamadzadeh, S. Bavari, and A. Schmaljohn.** 2003. Ebola and Marburg viruses replicate in monocyte-derived dendritic cells without inducing the production of cytokines and full maturation. J. Infect. Dis. **188:**1630–1638.
8. **Christensen, J. E., C. de Lemos, T. Moos, J. P. Christensen, and A. R. Thomsen.** 2006. CXCL10 is the key ligand for CXCR3 on $CD8^+$ effector T cells involved in immune surveillance of the lymphocytic choriomeningitis virus-infected central nervous system. J. Immunol. **176:**4235–4243.
9. **Chung, S. K., J. Y. Kim, I. B. Kim, S. I. Park, K. H. Paek, and J. H. Nam.** 2005. Internalization and trafficking mechanisms of coxsackievirus B3 in HeLa cells. Virology **333:**31–40.
10. **Colonna, M., G. Trinchieri, and Y. J. Liu.** 2004. Plasmacytoid dendritic cells in immunity. Nat. Immunol. **5:**1219–1226.
11. **den Haan, J. M., and M. J. Bevan.** 2002. Constitutive versus activation-dependent cross-presentation of immune complexes by $CD8^+$ and $CD8^-$ dendritic cells in vivo. J. Exp. Med. **196:**817–827.
12. **Diebold, S. S., T. Kaisho, H. Hemmi, S. Akira, and Reis e Sousa.** 2004. Innate antiviral responses by means of TLR7-mediated recognition of single-stranded RNA. Science **303:**1529–1531.
13. **Dufour, J. H., M. Dziejman, M. T. Liu, J. H. Leung, T. E. Lane, and A. D. Luster.** 2002. IFN-gamma-inducible protein 10 (IP-10; CXCL10)-deficient mice reveal a role for IP-10 in effector T cell generation and trafficking. J. Immunol. **168:**3195–3204.
14. **Edwards, A. D., S. S. Diebold, E. M. Slack, H. Tomizawa, H. Hemmi, T. Kaisho, S. Akira, and Reis e Sousa.** 2003. Toll-like receptor expression in murine DC subsets: lack of TLR7 expression by $CD8\alpha^+$ DC correlates with unresponsiveness to imidazoquinolines. Eur. J. Immunol. **33:**827–833.
15. **Egger, D., R. Gosert, and K. Bienz.** 2002. Role of cellular structures in viral RNA replication, p. 247–254. *In* B. Semler and E. Wimmer (ed.), Molecular biology of picornaviruses. ASM Press, Washington, DC.
16. **Fuse, K., G. Chan, Y. Liu, P. Gudgeon, M. Husain, M. Chen, W. C. Yeh, S. Akira, and P. P. Liu.** 2005. Myeloid differentiation factor-88 plays a crucial role in the pathogenesis of coxsackievirus B3-induced myocarditis and influences type I interferon production. Circulation **112:**2276–2285.
17. **Hardarson, H. S., J. S. Baker, Z. Yang, E. Purevjav, C. H. Huang, L. Alexopoulou, N. Li, R. A. Flavell, N. E. Bowles, and J. G. Vallejo.** 2007. Toll-like receptor 3 is an essential component of the innate stress response in virus-induced cardiac injury. Am. J. Physiol. Heart Circ. Physiol. **292:**H251–H258.
18. **Ho, L. J., J. J. Wang, M. F. Shaio, C. L. Kao, D. M. Chang, S. W. Han, and J. H. Lai.** 2001. Infection of human dendritic cells by dengue virus causes cell maturation and cytokine production. J. Immunol. **166:**1499–1506.
19. **Hsieh, M. F., S. L. Lai, J. P. Chen, J. M. Sung, Y. L. Lin, B. A. Wu-Hsieh, C. Gerard, A. Luster, and F. Liao.** 2006. Both CXCR3 and CXCL10/IFN-inducible protein 10 are required for resistance to primary infection by dengue virus. J. Immunol. **177:**1855–1863.
20. **Inaba, K., M. Inaba, N. Romani, H. Aya, M. Deguchi, S. Ikehara, S. Muramatsu, and R. M. Steinman.** 1992. Generation of large numbers of dendritic cells from mouse bone marrow cultures supplemented with granulocyte/macrophage colony-stimulating factor. J. Exp. Med. **176:**1693–1702.
21. **Kandolf, R., and P. H. Hofschneider.** 1985. Molecular cloning of the genome of a cardiotropic coxsackie B3 virus: full-length reverse-transcribed recombinant cDNA generates infectious virus in mammalian cells. Proc. Natl. Acad. Sci. USA **82:**4818–4822.
22. **Kandolf, R., M. Sauter, C. Aepinus, J. J. Schnorr, H. C. Selinka, and K. Klingel.** 1999. Mechanisms and consequences of enterovirus persistence in cardiac myocytes and cells of the immune system. Virus Res. **62:**149–158.
23. **Kaya, Z., K. M. Dohmen, Y. Wang, J. Schlichting, M. Afanasyeva, F. Leuschner, and N. R. Rose.** 2002. Cutting edge: a critical role for IL-10 in induction of nasal tolerance in experimental autoimmune myocarditis. J. Immunol. **168:**1552–1556.
24. **Khan, I. A., J. A. MacLean, F. S. Lee, L. Casciotti, E. DeHaan, J. D. Schwartzman, and A. D. Luster.** 2000. IP-10 is critical for effector T cell trafficking and host survival in Toxoplasma gondii infection. Immunity **12:**483–494.
25. **Klingel, K., C. Hohenadl, A. Canu, M. Albrecht, M. Seemann, G. Mall, and R. Kandolf.** 1992. Ongoing enterovirus-induced myocarditis is associated with persistent heart muscle infection: quantitative analysis of virus replication, tissue damage, and inflammation. Proc. Natl. Acad. Sci. USA **89:**314–318.
26. **Klingel, K., J. J. Schnorr, M. Sauter, G. Szalay, and R. Kandolf.** 2003. β2-microglobulin-associated regulation of interferon-gamma and virus-specific immunoglobulin G confer resistance against the development of chronic coxsackievirus myocarditis. Am. J. Pathol. **162:**1709–1720.
27. **Klingel, K., S. Stephan, M. Sauter, R. Zell, B. M. McManus, B. Bultmann, and R. Kandolf.** 1996. Pathogenesis of murine enterovirus myocarditis: virus dissemination and immune cell targets. J. Virol. **70:**8888–8895.
28. **Law, H. K., C. Y. Cheung, H. Y. Ng, S. F. Sia, Y. O. Chan, W. Luk, J. M. Nicholls, J. S. Peiris, and Y. L. Lau.** 2005. Chemokine up-regulation in SARS-coronavirus-infected, monocyte-derived human dendritic cells. Blood **106:**2366–2374.
29. **Losana, G., C. Bovolenta, L. Rigamonti, I. Borghi, F. Altare, E. Jouanguy, G. Forni, J. L. Casanova, B. Sherry, M. Mengozzi, G. Trinchieri, G. Poli, F. Gerosa, and F. Novelli.** 2002. IFN-gamma and IL-12 differentially regulate CC-chemokine secretion and CCR5 expression in human T lymphocytes. J. Leukoc. Biol. **72:**735–742.
30. **Makino, Y., D. N. Cook, O. Smithies, O. Y. Hwang, E. G. Neilson, L. A. Turka, H. Sato, A. D. Wells, and T. M. Danoff.** 2002. Impaired T cell function in RANTES-deficient mice. Clin. Immunol. **102:**302–309.
31. **Maldonado-Lopez, R., T. De Smedt, B. Pajak, C. Heirman, K. Thielemans, O. Leo, J. Urbain, C. R. Maliszewski, and M. Moser.** 1999. Role of $CD8\alpha^+$ and $CD8\alpha^-$ dendritic cells in the induction of primary immune responses in vivo. J. Leukoc. Biol. **66:**242–246.
32. **Marshall-Clarke, S., J. E. Downes, I. R. Haga, A. G. Bowie, P. Borrow, J. L. Pennock, R. K. Grencis, and P. Rothwell.** 2007. Polyinosinic acid is a ligand for toll-like receptor 3. J. Biol. Chem. **282:**24759–24766.
33. **Melnick, J. L.** 1996. Enteroviruses: poliovirus, coxsackieviruses, echoviruses,

and newer enteroviruses, p. 655–712. *In* B. N. Fields, D. M. Knipe, and P. Howley (ed.), Fields virology, 3rd ed. Lippincott-Raven, New York, NY.

34. **O'Keeffe, M., H. Hochrein, D. Vremec, I. Caminschi, J. L. Miller, E. M. Anders, L. Wu, M. H. Lahoud, S. Henri, B. Scott, P. Hertzog, L. Tatarczuch, and K. Shortman.** 2002. Mouse plasmacytoid cells: long-lived cells, heterogeneous in surface phenotype and function, that differentiate into $CD8^+$ dendritic cells only after microbial stimulus. J. Exp. Med. **196:**1307–1319.
35. **O'Keeffe, M., H. Hochrein, D. Vremec, B. Scott, P. Hertzog, L. Tatarczuch, and K. Shortman.** 2003. Dendritic cell precursor populations of mouse blood: identification of the murine homologues of human blood plasmacytoid pre-DC2 and $CD11c^+$ DC1 precursors. Blood **101:**1453–1459.
36. **Ostrowski, M., M. Vermeulen, O. Zabal, J. R. Geffner, A. M. Sadir, and O. J. Lopez.** 2005. Impairment of thymus-dependent responses by murine dendritic cells infected with foot-and-mouth disease virus. J. Immunol. **175:** 3971–3979.
37. **Pooley, J. L., W. R. Heath, and K. Shortman.** 2001. Cutting edge: intravenous soluble antigen is presented to CD4 T cells by CD8- dendritic cells, but cross-presented to CD8 T cells by $CD8^+$ dendritic cells. J. Immunol. **166:** 5327–5330.
38. **Proietto, A. I., M. O'Keeffe, K. Gartlan, M. D. Wright, K. Shortman, L. Wu, and M. H. Lahoud.** 2004. Differential production of inflammatory chemokines by murine dendritic cell subsets. Immunobiology **209:**163–172.
39. **Rudd, B. D., E. Burstein, C. S. Duckett, X. Li, and N. W. Lukacs.** 2005. Differential role for TLR3 in respiratory syncytial virus-induced chemokine expression. J. Virol. **79:**3350–3357.
40. **Schulz, O., S. S. Diebold, M. Chen, T. I. Naslund, M. A. Nolte, L. Alexopoulou, Y. T. Azuma, R. A. Flavell, P. Liljestrom, and Reis e Sousa.** 2005. Toll-like receptor 3 promotes cross-priming to virus-infected cells. Nature **433:**887–892.
41. **Shortman, K., and Y. J. Liu.** 2002. Mouse and human dendritic cell subtypes. Nat. Rev. Immunol. **2:**151–161.
42. **Steinman, R. M., and M. Pope.** 2002. Exploiting dendritic cells to improve vaccine efficacy. J. Clin. Investig. **109:**1519–1526.
43. **Szalay, G., M. Sauter, J. Hald, A. Weinzierl, R. Kandolf, and K. Klingel.** 2006. Sustained nitric oxide synthesis contributes to immunopathology in ongoing myocarditis attributable to interleukin-10 disorders. Am. J. Pathol. **169:**2085–2093.
44. **Takeda, K., and S. Akira.** 2005. Toll-like receptors in innate immunity. Int. Immunol. **17:**1–14.
45. **Wang, J. P., D. R. Asher, M. Chan, E. A. Kurt-Jones, and R. W. Finberg.** 2007. Cutting edge: antibody-mediated TLR7-dependent recognition of viral RNA. J. Immunol. **178:**3363–3367.
46. **Wessely, R., K. Klingel, K. U. Knowlton, and R. Kandolf.** 2001. Cardioselective infection with coxsackievirus B3 requires intact type I interferon signaling: implications for mortality and early viral replication. Circulation **103:**756–761.
47. **Yoneyama, H., S. Narumi, Y. Zhang, M. Murai, M. Baggiolini, A. Lanzavecchia, T. Ichida, H. Asakura, and K. Matsushima.** 2002. Pivotal role of dendritic cell-derived CXCL10 in the retention of T helper cell 1 lymphocytes in secondary lymph nodes. J. Exp. Med. **195:**1257–1266.
48. **Zhang, H. M., J. Yuan, P. Cheung, D. Chau, B. W. Wong, B. M. McManus, and D. Yang.** 2005. Gamma interferon-inducible protein 10 induces HeLa cell apoptosis through a p53-dependent pathway initiated by suppression of human papillomavirus type 18 E6 and E7 expression. Mol. Cell. Biol. **25:** 6247–6258.